MICHIGAN STATE UNIVERSITY

CYCLOTRON LABORATORY

STUDY OF FAST PARTICLE EMISSION FROM HEAVY ION INDUCED REACTIONS

C.K. GELBKE

INVITED TALK GIVEN AT THE WORKSHOP ON COINCIDENT PARTICLE EMISSION FROM CONTINUUM STATES, BAD HONNEF 4-7 JUNE 1984

JULY 1984

MSUCL-472

MSUCL-472
July 1984

STUDY OF FAST PARTICLE EMISSION FROM HEAVY ION INDUCED REACTIONS

C.K. Gelbke

Department of Physics and Astronomy and
National Superconducting Cyclotron Laboratory
Michigan State University, East Lansing, MI 48824,USA

1. Introduction

Perhaps one of the most interesting open problems in nuclear physics concerns the question whether it is possible to extract information about the thermodynamic properties of nuclear matter from nuclear collision experiments. This question cannot be answered trivially because of several complications which arise from the fact that nuclear collision experiments correspond to the formation and decay of short lived nuclear systems which contain less than 500 nucleons: (i) Because of the finite number of particles, thermodynamic quantities may not be sharply defined and may be associated with sizeable fluctuations; the phase space constraints imposed by conservation laws have to be understood in detail and included into theories which are capable of predicting multiparticle observables. (ii) Because of the small size of the reaction volume, surface effects may introduce considerable deviations from the thermodynamic behavior of bulk nuclear matter. (iii) Because of the small containment times, statistical equilibrium may not be achieved and the reaction dynamics may have to be understood in considerable detail before information about the thermodynamic properties of nuclear matter may be extracted from experimental observations.

Recent theoretical investigations indicate that nuclear matter should exist in the liquid and gaseous phases. As an example, Figure 1 shows a pressure vs. density phase diagram of nuclear matter calculated[1]) with a Skyrme-type interaction. For temperatures lower than the critical temperature T_c=20 MeV, the liquid and gaseous phases coexist over a certain range of density (see hatched area). At the critical temperature, liquid and gaseous phases can only coexist at the critical density ρ_c=0.07 fm^{-3}. At higher temperatures only the gas phase exists. Although the qualitative features of the phase diagram shown in Figure 1 are most likely correct, the numerical values of the critical temperature and density have considerable uncertainties.

INFORMATION ABOUT EXTREME STATES OF NUCLEAR MATTER FROM NUCLEAR COLLISION EXPERIMENTS?

$1 << N << \infty$: FLUCTUATIONS
CONSTRAINTS FROM CONSERVATION LAWS
SURFACE EFFECTS
SMALL CONTAINMENT TIMES (TRANSIENTS?)
REACTION DYNAMICS

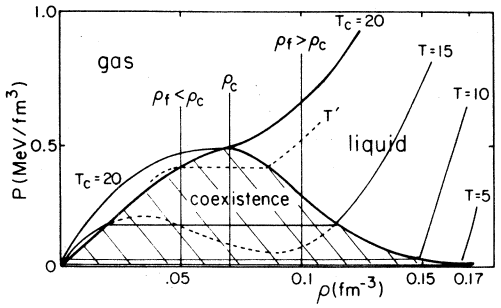

Fig.1 Diagram of pressure versus density for nuclear matter as calculated[1]) with a Skyrme-type interaction. List of problems concerning the interpretation of nuclear collision experiments in terms of the properties of infinite nuclear matter.

Heavy ion induced reactions at intermediate energies (E/A≈20-200 MeV) may be ideally suited to investigate the important question whether nuclear collision experiments may, indeed, provide information about the nuclear equation of state. Theoretically, there is little doubt that a liquid gas phase transition should exist for nuclear matter at moderate temperatures and, experimentally, the appropriate range of temperatures is accessible - provided that at least local thermal equilibrium is reached in these collisions and that statistical concepts are still useful. I want to point out that rather similar questions will have to be addressed at much higher energies

where the transition to the quark gluon plasma is expected to take place.

In this talk I will not try to address the difficult question whether and how the liquid gas phase diagram may be related to observables of a nuclear collision experiment. The answer to this question is not yet known - see the stimulating contribution by P. Siemens to this conference. Rather, I would like to summarize recent experimental results and discuss the question whether existing experimental information may be understood in terms of statistical concepts. I would like to stress that my discussion of the data will be rather schematic. Instead of trying to do justice to the full complexity of the nuclear collision process I will use some very simple parameterisations to illustrate certain physical effects. In the absence of a more complete and reliable theory, such an approach is useful since it allows the organization of large amounts of data in terms of a few parameters. These parameterisations have to be taken with a grain of salt and should not be over-interpreted.

2. Incomplete Fusion

For intermediate energy nucleus nucleus collisions the relative velocity of the two colliding nuclei is comparable or may exceed the Fermi velocity and the velocity of sound. As a consequence, individual nucleon nucleon collisions should become more important and mean field aspects should cease to dominate the reaction mechanism.

At low projectile energies of only a few MeV per nucleon above the Coulomb barrier, central collisions are generally associated with the complete fusion of projectile and target nuclei leading to the formation of a compound nucleus. After reaching full statistical equilibrium of its intrinsic degrees of freedom, the compound nucleus decays by light particle evaporation, Y-ray emission or fission. At higher energies, particle emission prior to the attainment of full statistical equilibrium of the composite nucleus becomes important.

Since these particles have forward peaked angular distributions in the center-of-mass frame, the average velocity of the remaining heavy composite system (which evolves towards equilibrium) is smaller than the velocity of the center-of-mass system. These reaction are also referred to as incomplete fusion reactions or incomplete momentum transfer reactions, since neither the entire projectile mass nor the entire projectile momentum have been absorbed by the remaining heavy residue.

Information about the relative importance of complete and incomplete fusion reactions may be obtained by measuring the recoil velocity of the remaining heavy residual nucleus[2,3]) or, for fissionable nuclei, by measuring the folding angle θ_{AB} between two coincident fission fragments resulting from the fission decay of the heavy residual nucleus[4–6]). The latter method is illustrated in Figure 2. Increasing linear momentum transfers correspond to smaller folding angles. By means of this technique it is also possible to distinguish

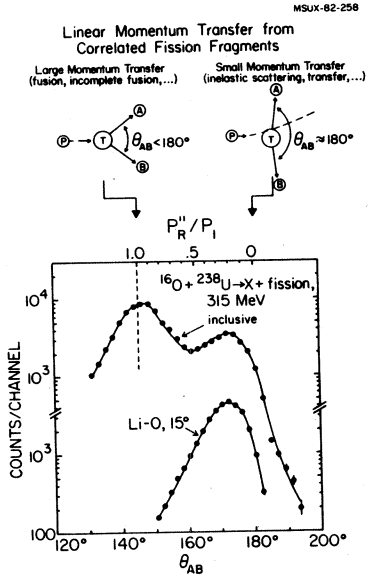

Fig.2 Information about linear momentum transfer from folding angle measurements for correlated fission fragments. Folding angle distributions measured for ^{16}O induced reactions on ^{238}U at 310 MeV[7]).

"central" or fusion-like reactions from "peripheral" or transfer-like reactions for which projectile-like fragments emerge in the exit channel[7]).

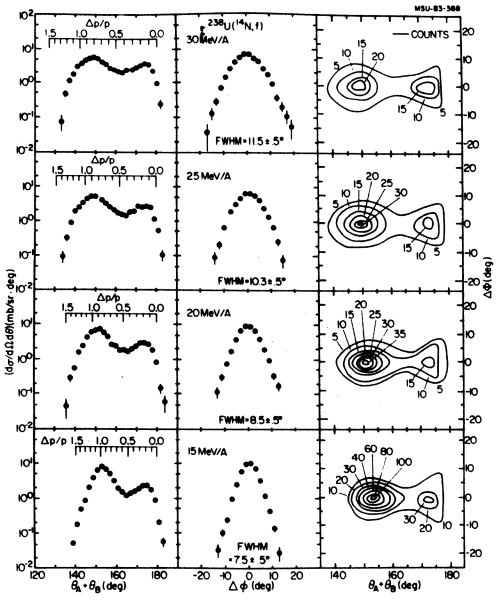

Fig.3 Folding angle distributions between coincident fission fragments measured [6]) for ^{14}N induced reactions on ^{238}U at E/A=15, 20, 25, and 30 MeV.

Figure 3 shows the folding angle distributions measured[6]) for ^{14}N induced reactions on ^{238}U at the incident energies of E/A=15, 20, 25, and 30 MeV. In the figure, θ_A and θ_B denote the laboratory angles of the two coincident fission fragments measured with respect to the beam axis and $\Delta\phi$ denotes the angle between the two planes defined by the beam axis in combination with either of the fission fragment velocity vectors. The right hand column of the figure shows contour plots of the number of coincident events in a $\theta_A+\theta_B$ versus $\Delta\phi$ plane. The two peaks corresponding to (i) large momentum transfer or fusion-like reactions, and (ii) small momentum transfer or transfer-like reactions can be clearly distinguished. The center column of the figure shows the out-of-plane distributions for fusion like reactions. The widths

of these out-of-plane distributions increase significantly with incident energy in accordance with an increase in the emission of light particles at higher energies. The left hand column of the figure shows the dependence of the fission cross sections on the folding angle $\theta_A+\theta_B$. The upper scales show the average recoil momentum Δp of the fissioning nucleus in units of the projectile momentum p. For fusion-like reactions at higher projectile energies, smaller fractions of the projectile momentum are transferred to the fissioning nucleus, reflecting the increasing importance of light particle emission prior to the attainment of full statistical equilibrium of the composite nucleus.

Because of the broadening of the folding angle distributions by light particle emission it is not possible to separate complete and incomplete fusion reactions. It is, however, possible to estimate an upper limit for the contribution of complete fusion to all of the fusion-like processes. Figure 4 shows the energy dependence of the ratio σ_{CF}/σ_{FL}, where σ_{CF} denotes the estimated upper limit for the fission cross section following complete fusion reactions and σ_{FL} denotes the fission cross section following fusion-like reactions. The figure clearly demonstrates the decreasing importance of complete

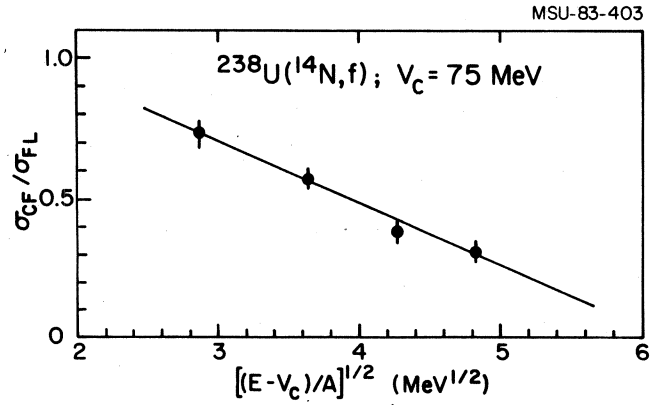

Fig.4 Estimated upper limit for the contribution of complete fusion to the fission cross section corresponding to fusion-like reactions for ^{14}N induced reactions on ^{238}U[6]).

fusion reactions at higher projectile energies. An extrapolation of these data suggests that complete fusion reactions will cease to contribute at incident energies above E/A=40-45 MeV[6]).

3. Non-compound light particle emission

Because of momentum conservation, the reduced recoil velocities of the composite nucleus formed in fusion-like reactions must be accompanied by particle emission with forward peaked angular distributions. Figure 5 shows neutron spectra measured[8]) in coincidence with fission fragments for ^{16}O induced reactions on ^{238}U at the incident energy of 310 MeV. The energy spectra clearly exhibit two components. The low energy component may be understood in terms of neutron evaporation from the compound nucleus and from the fully

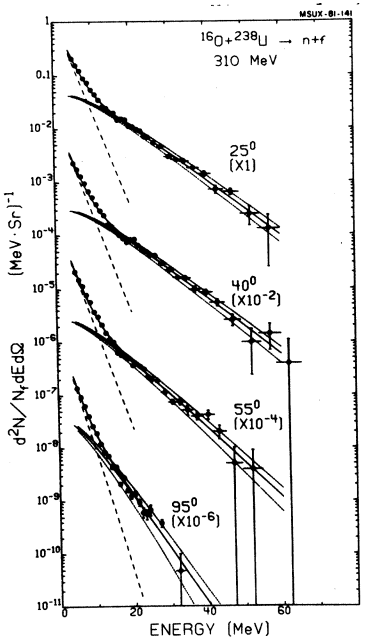

Fig.5 Differential neutron multiplicities per fission event measured for the reaction $^{238}U(^{16}O,nf)$ at 310 MeV. The dashed and solid lines show the decomposition into equilibrium and non-equilibrium components, respectively[8]).

accelerated fission fragments. The high energy component, on the other hand, is due to neutron emission prior to the attainment of full statistical equilibrium. For the $^{16}O+^{238}U$ reaction, the deexcitation of fully equilibrated reaction products (compound nucleus or fission fragments) occurs primarily via neutron emission. For charged particle emission, the equilibrium component is strongly reduced in magnitude as compared to the non-equilibrium component[9]), see also Figs.7 and 25, below. Because of obvious experimental advantages, emission prior to the attainment of full statistical equilibrium has been primarily investigated for the emission of charged particles.

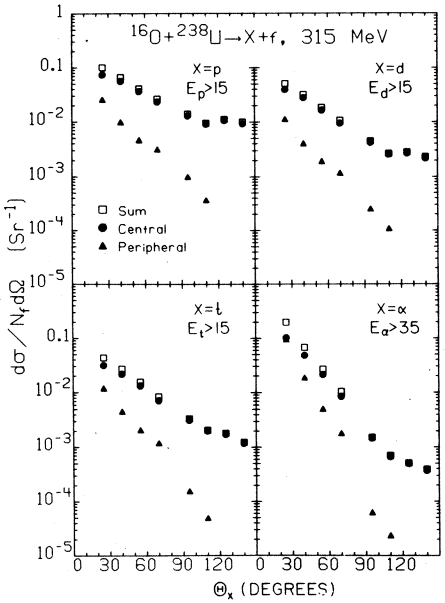

Fig.6 Angular distributions of protons, deuterons, tritons and alpha particles measured for ^{16}O induced reactions on ^{238}U. Fusion-like or "central" collisions and transfer-like or "peripheral" collisions are defined by $\Delta p/p>0.5$ and $\Delta p/p<0.5$, respectively.

Figure 6 shows the angular distributions of protons, deuterons, tritons, and alpha particles measured in coincidence with fission fragments for ^{16}O induced reactions on ^{238}U at 310 MeV[9]). The circular points correspond to particle emission in "central" or fusion-like

reactions (defined by $\Delta p/p>0.5$) and the triangular points correspond to particle emission in "peripheral" or transfer-like reactions (defined by $\Delta p/p<0.5$); the sum of the two contributions is given by the open squares. Light particles emitted at forward angles are emitted in both fusion-like and transfer-like reactions. With increasing detection angle, the relative contribution of transfer-like "peripheral" collisions decreases rapidly as compared to the contribution from fusion-like "central" collisions. Except at very forward angles, the cross sections for non-compound light particle emission are dominated by fusion-like reactions. At forward angles, the relative contributions from transfer-like reactions are largest for alpha particle emission as compared to the emission of protons, deuterons and tritons. Since the relatively trivial processes of quasi-elastic projectile breakup and statistical decay of excited projectile residues are expected to contribute to transfer-like reactions (but not to fusion-like reactions), particle emission prior to the attainment of full statistical equilibrium may best be studied at intermediate angles or by requiring coincidences with fusion-like events (see also the interesting contribution by D. Hilscher to this conference).

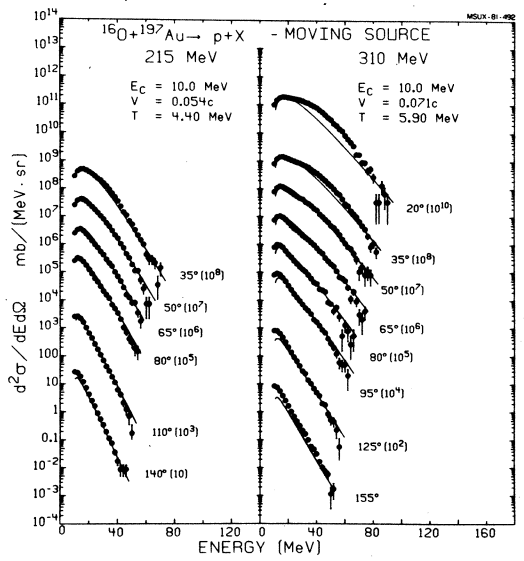

Fig.7 Energy spectra measured for the reaction $^{197}Au(^{16}O,p)$ at E/A= 13.4 and 19.4 MeV. The solid lines are fit to the data using the simple moving source parameterization including the effect of Coulomb repulsion from the target residue[10].

Figure 7 shows single particle inclusive proton cross sections measured[10]) for ^{16}O induced reactions on ^{197}Au at the incident energies of 215 and 310 MeV. With the exception of the most forward and most backward angles, the energy spectra may be rather well described in terms of a Maxwellian distribution centered about a velocity v_o that is, in general, slightly less than half the beam velocity[10]). The nonrelativistic expression of the laboratory cross sections is given by

$$\frac{d^2\sigma}{d\Omega dE} = \text{const } E^{1/2} \exp\{-(E+E_o-2E^{1/2}E_o^{1/2}\cos\theta)/T\} \qquad (1)$$

where $E_o=mv_o^2/2$; T is temperature parameter which characterizes the width of the velocity distribution; E and m are the energy and mass of the detected particle. Coulomb repulsion from a stationary target nucleus may be approximated[9]) by replacing E by $E-E_c$, where E_c is the kinetic energy gained by the particle due to Coulomb repulsion from the target. Except at very forward angles, the emission of energetic light particles is largely associated with fusion-like reactions for which nearly the entire projectile is absorbed by the target nucleus. Therefore, this "moving source" parameterization must not[10]) be interpreted in terms of a hot gas of nucleons separated from the target nucleus. It simply indicates that the inclusive cross sections may be rather well described in terms of a random velocity distribution centered about a mean velocity which is different from the velocity of the compound nucleus. The inclusive cross sections do not contain significant additional information. Since the mean velocity of the single particle distribution is generally found to be slightly less than half the beam velocity it is plausible that noncompound light particle emission takes place at the early stages of the reaction and involves the interaction of only a subset of nucleons. Whether the apparent random character of the single particle inclusive velocity distribution reflects the averaging over many different reaction channels, whether it may be interpreted in terms of direct knockout[10,11]) or fusion-breakup processes[12,13]), or whether it

reflects statistical emission processes from subsets of nucleons, is clearly an important question which will have to be addressed in more detailed coincidence experiments.

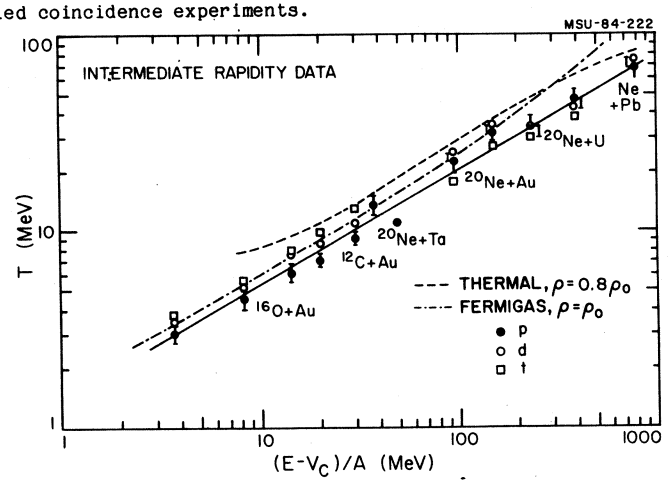

Fig.8 Energy dependence of temperature parameter T extracted from fits to light particle inclusive cross sections measured for ^{12}C, ^{16}O, and ^{20}Ne induced reactions on heavy targets. The curves shown in the figure are explained in the text.

Although the moving source parameterisation is not unique and slightly different parameterisations may be used to characterize the single particle distributions, it may be used to characterize the essential features of noncompound light particle emission over a large range of projectile energies in terms of a few parameters[10,14]. Figure 8 shows the energy dependence of the temperature parameter T characterizing the light particle spectra for ^{12}C, ^{16}O, and ^{20}Ne induced reactions on heavy targets over a wide range of energies. To minimize contributions from projectile breakup and from the statistical decay of excited projectile and target residues, only those particles were included in the analysis which were emitted at laboratory angles larger than about 40° and with energies above the ones expected from compound nucleus evaporation. The extracted temperature parameters exhibit a smooth energy dependence

corresponding to an approximate power law as is shown by the solid line. For orientation, the dot-dashed curve corresponds to the temperature of an ideal Fermi gas of normal nuclear density consisting of equal numbers of projectile and target nucleons. Except for the highest energies, for which cooling by pion production is expected to become important, this curve follows the trend of the data rather well. The dashed curve corresponds to calculations for a free, strongly interacting gas in thermal and chemical equilibrium as predicted by the fireball model[15,16] for the impact parameter of maximum weight assuming a freeze-out density of ρ_f=0.8 ρ_o=0.12 fm^{-3}; these calculations take the effect of cooling by particle production into account.

4. The assumption of local statistical equilibrium

The systematic variation of the temperature parameter over a large range of projectile energies and the similarities of the temperature parameters extracted for different light particles may indicate that single particle observables are rather insensitive to the detailed dynamics of the reaction and that they are dominated by the available phase space. Since statistical equilibrium is not reached for the entire composite system, the assumption of statistical emission from a subset of nucleons may be a useful working hypothesis. One may then proceed in two directions: (i) investigate whether a larger body of single-particle inclusive data may be understood in terms of a consistent set of assumptions and (ii) perform more detailed coincidence experiments in order to test whether many-particle observables may still be understood in terms of statistical arguments or whether new dynamical effects have to be included into theoretical descriptions of the data.

At present, a realistic theory for noncompound particle emission in intermediate energy nucleus nucleus collisions is not available. The formulation of such a theory is clearly a nontrivial task which

has to be undertaken in the future. In the meantime, we will have to be content with more schematic model calculations which may be used to illustrate certain effects.

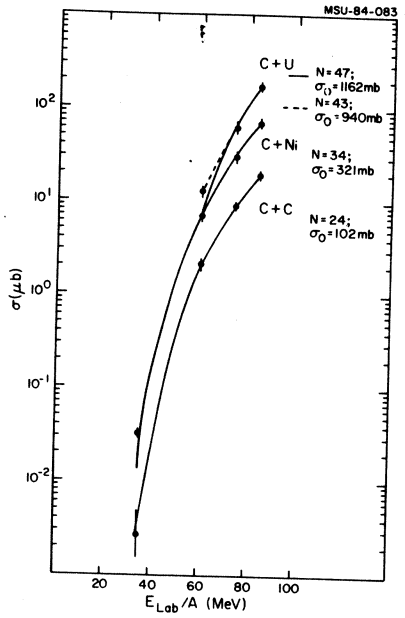

Fig.9 Energy dependence of inclusive total π_o cross sections for ^{12}C induced reactions on C, Ni, and U. The solid curves correspond to Hauser Feshbach type calculations generalized for the decay of a hot spot[19]).

As has been discussed previously[17]), statistical model calculations can reproduce the relative abundance of protons, deuterons, tritons, and alpha particles over a large range of energies. More recent statistical calculations have also been able to reproduce the energy dependence of "subthreshold" pion production cross sections[18-20]). As an example, Figure 9 shows the energy dependence of the total inclusive π_o cross sections for ^{12}C induced reactions on targets of C, Ni and U. The solid curves[19]) correspond to statistical calculations based on the Weisskopf formula which was modified to include the decay of a "hot spot". The calculations can reproduce the energy dependence of the cross sections rather well. Similar agreement was obtained with an alternative statistical

model[20]) in which the geometrical and statistical aspects the reaction were treated differently. Common to both approaches is the assumption that only subsets of nucleons participate in the process leading to the statistical emission of "subthreshold" pions.

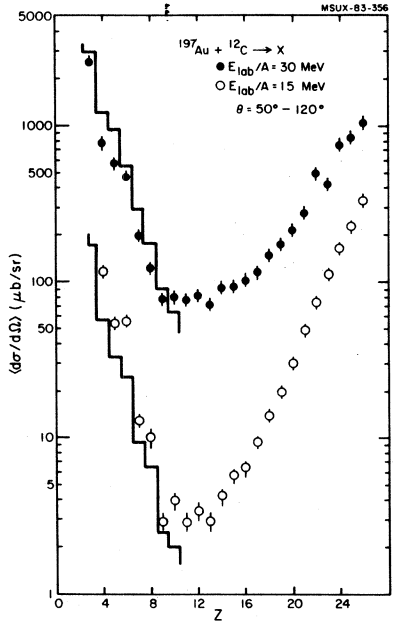

Fig.10 Angle averaged element cross sections for ^{12}C induced reactions on ^{197}Au at E/A=15 and 30 MeV. The histograms show the relative yields expected for the decay of the compound nucleus[23]).

Statistical model calculations[21,22]) have predicted non-negligible probabilities for the emission of complex nuclei (Z>2). The emission of these nuclei is predicted to be favored at moderate temperatures of about 5-10 MeV and should, therefore, be observable in intermediate energy nucleus nucleus collisions. A recent measurement performed at Michigan State University has verified this qualitative prediction. Figure 10 shows the angle averaged cross sections for the emission of complex nuclei at angles significantly larger than the grazing angle measured[23]) for ^{12}C induced reactions on ^{197}Au at E/A=15 and 30 MeV. Over this energy range, the cross sections leading to the emission of fragments with element numbers 2<Z<16 increase by more

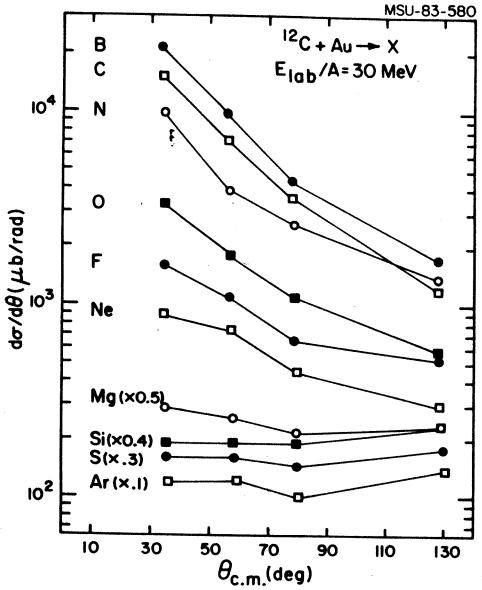

Fig.11 Energy integrated angular distribution of several complex fragments emitted in ^{12}C induced reactions on ^{197}Au E/A=30 MeV[24]).

than one order of magnitude. The large cross sections for elements heavier than sulphur correspond, most likely, to the extreme tails of the element distribution resulting from fission of the composite nucleus or the target residue. It is quite clear that the rapid rise of the cross sections for elements lighter than Z=10 cannot be interpreted in terms of conventional fission. Figure 11 shows the energy integrated angular distributions for several fragments with 4<Z<20. For lighter elements, the angular distributions are forward peaked indicating that these elements are emitted prior to the attainment of full statistical equilibrium of the composite nucleus. With increasing element number the angular distributions become less forward peaked indicating higher degrees of equilibration of the emitting system.

The energy spectra of fragments with Z=5-10 emitted in ^{12}C induced reactions on ^{197}Au at E/A=30 MeV are shown in Figure 12. At each scattering angle the energy spectra exhibit approximately

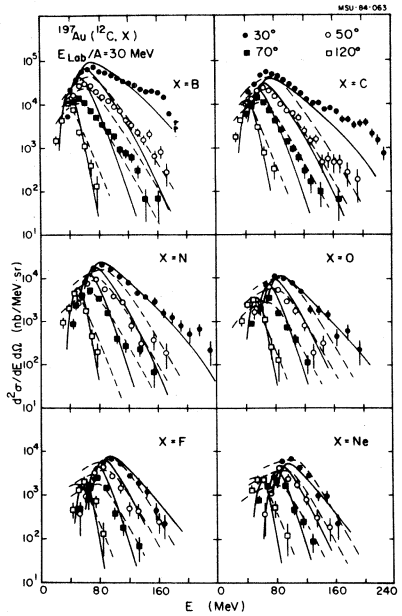

Fig.12 Differential cross sections for the emission of complex nuclei measured for ^{12}C induced reactions on ^{197}Au at E/A=30 MeV. The solid and dashed curves are calculated by assuming emission from a hot spot and the shattering of the cold target spectator matter, respectively[24]).

exponential slopes which become steeper at more backward angles. At present, the reaction mechanism leading to the emission of complex fragments is not fully understood. The solid and dashed lines shown in the figure are the results of two different model calculations[24]) which are illustrated by the schematic diagram given in Figure 13. Both models assume the formation and decay of a localized region of high excitation ("hot spot"). In the calculations shown by the solid lines it is assumed that complex nuclei are emitted from the hot spot which is assumed to cool by particle emission and by the simultaneous accretion of nucleons from the cold spectator matter. Particle emission rates are calculated from a generalized Weisskopf formula using a modified version of the program by Friedman and Lynch[22]). The calculations shown by the dashed lines, on the other hand, assume that complex fragments result from the random shattering of the cold spectator matter which is destabilized by the passage of energetic

Emission of Intermediate Mass Fragments

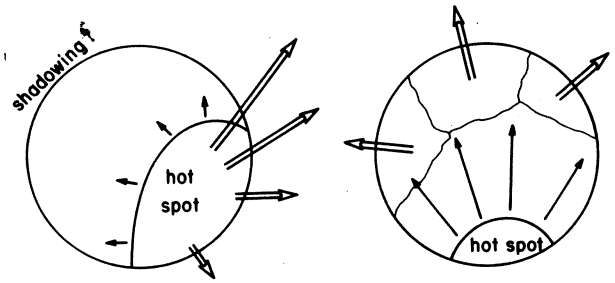

Fig.13 Schematic illustration of two alternative interpretations of the reaction mechanism leading to the emission of complex nuclei prior to the attainment of full statistical equilibrium of the composite nucleus.

nucleons originating from the hot spot. Both models can reproduce the qualitative trends of the differential cross sections rather well. In both models, the formation of a localized region of high excitation is assumed for the early stages of the reaction. However, entirely different assumptions are made for the decay of this initial hot spot and the process leading to the emission of complex fragments.

These examples should suffice to illustrate that single particle inclusive observables may be rather successfully described in terms of statistical models which are based on the assumption that only subsets of nucleons participate at the early stages of the reactions and that the phase space available for these subsets is uniformly populated. Future investigations should address the question whether any of the proposed statistical models can give a consistent description of the the emission of many different particles, ranging from pions to complex nuclei. Ultimately, however, single particle observables are not expected to contain sufficient information to elucidate more detailed dynamical aspects of the collision process. Many of the open questions will have to be addressed by more restrictive coincidence experiments.

Space-Time Dimensions of Thermal Systems

$$\frac{\sigma_2(\vec{p}_1,\vec{p}_2)}{\sigma_1(\vec{p}_1)\,\sigma_1(\vec{p}_2)} = N\left[1+R(\vec{p}_1,\vec{p}_2)\right] \quad , \quad R(\vec{p}_1,\vec{p}_2) = \frac{1}{(2\pi)^{3/2}\, r_0^2\, \rho} \int d^3r \, \exp\left[\frac{(\vec{r}\,\vec{v}'\tau/\rho)^2 - r^2}{2r_0^2}\right]$$

$$\times \left\{\frac{1}{4}\left|{}^1\psi_{\Delta p}(\vec{r})\right|^2 + \frac{3}{4}\left|{}^3\psi_{\Delta p}(\vec{r})\right|^2 - 1\right\}$$

$$\vec{v}' = \frac{\vec{p}_1+\vec{p}_2}{2m} - \vec{v}_0 \; ; \; \rho = \left[r_0^2 + (\vec{v}'\tau)^2\right]^{1/2}$$

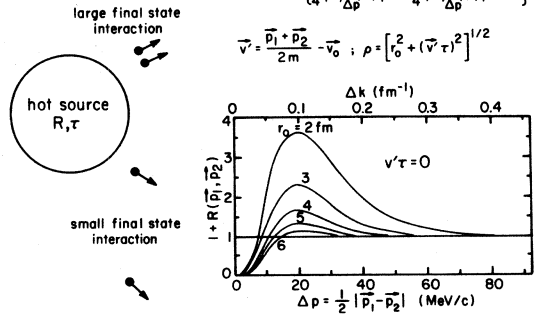

Fig.14 Schematic illustration of light particle correlations which may contain information about the space-time extent of incoherently radiating sources.

5. Light particle correlations at small relative momenta

The success of phase space models involving only subsets of nucleons raises the important question whether these subsets are merely linked by individual nucleon nucleon collisions or whether, in addition, they should be understood in terms of a spatially localized region of high excitation as is implied by the concept of a hot spot. Information about the space time extent of the emitting sources may be extracted from measurements of light particle correlations at small relative momenta[25,26]. The underlying principle is illustrated in Figure 14. If light particles are randomly emitted from a short-lived source of small spatial extent their wavepackets will overlap. As a result, the wavefunction describing the relative motion of the two particles reflects final state interactions[26] and quantum statistical effects[25]. For the case of two protons emitted at close proximity in space and time, the attractive nuclear interaction in the singlet s partial wave causes a characteristic enhancement in the two proton correlation at relative momenta of about 20 MeV/c. Emission from a

source or large dimensions or long lifetime will result in a reduced final-state effect. The curves shown in the figure illustrate the sensitivity of the correlation function to the spatial extent of the emitting source assuming negligible source lifetime and Gaussian spatial density distributions[26].

The two-particle correlation function, $R(\vec{p}_1,\vec{p}_2)$, is defined in terms of the singles cross sections, $\sigma(\vec{p}_1)$, $\sigma(\vec{p}_2)$, and the coincidence cross section, $\sigma(\vec{p}_1,\vec{p}_2)$, by

$$\sigma(\vec{p}_1,\vec{p}_2) = C\,\sigma(\vec{p}_1)\sigma(\vec{p}_2)[1+R(\vec{p}_1,\vec{p}_2)] \qquad (2)$$

where $\vec{p}_1$ and $\vec{p}_2$ denote the momenta of the two coincident particles; the normalization constant C is experimentally determined by the condition $R(\vec{p}_1,\vec{p}_2)=0$ for sufficiently large relative momenta, where final-state interactions are not important. For a source of negligible lifetime, $R(\vec{p}_1,\vec{p}_2)$ depends primarily on the magnitude of the relative momentum $\Delta\vec{p}=M(\vec{p}_1/m_1-\vec{p}_2/m_2)$, with $M=m_1m_2/(m_1+m_2)$.

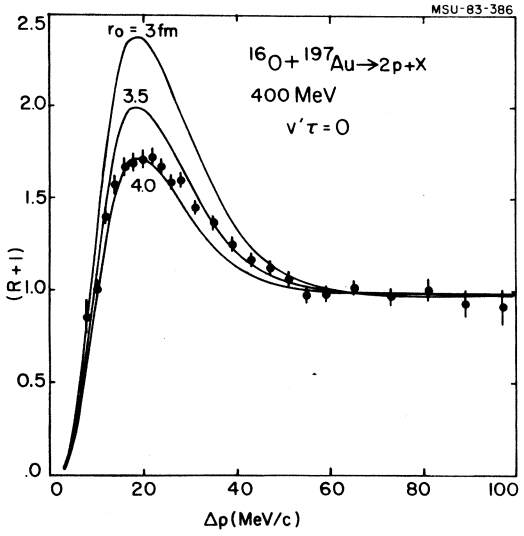

Fig.15 Two-proton correlation function measured[27] for ^{16}O induced reactions on ^{197}Au at E/A=15 MeV. The curves are the result of model calculations[26] for the case of incoherent emission from a source of negligible lifetime and Gaussian spatial distribution.

Figure 15 shows the experimental correlation function, 1 (Δp), measured[27] at an average laboratory angle of 15° for ^{16}O induced reactions on ^{197}Au at 400 MeV. This correlation function was obtained by inserting the measured cross sections into eq. (2) and by summing both sides of the equation over all energies and angles corresponding to a given relative momentum. The curves shown in the figure correspond to model calculations[26] for the case of incoherent emission from sources of negligible lifetime and Gaussian density distributions, $\rho(r)=\rho_o(-r^2/r_o^2)$. Since non-negligible decay times will reduce the calculated correlations, the value of r_o=4 fm deduced from the present calculations represents an upper limit on the average source size.

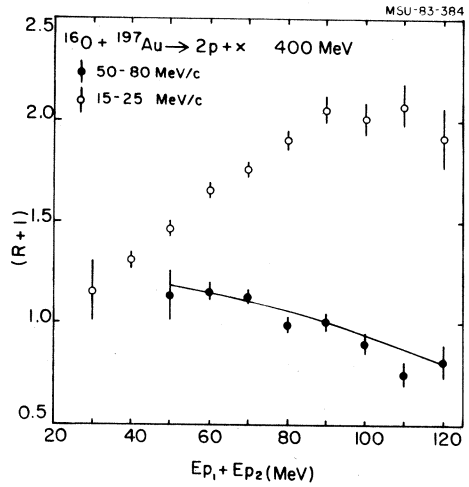

Fig.16 Dependence of the correlation function on the sum energy of the two coincident protons for the relative momentum intervals of 15-25 and 50-80 MeV/c[27].

Further insight may be gained[27] from the dependence of the measured correlations on the total energy of the two outgoing protons. This energy dependence is shown in Figure 16 for the relative momentum intervals of $\Delta_1 p$=15-25 MeV/c [where R(Δp) is predicted to reach its maximum] and $\Delta_2 p$=50-80 MeV/c [where R(Δp) is predicted to be negligible]. With increasing proton energies the differences between the correlations measured for the two momentum intervals become more

pronounced, indicating that high-energy protons are emitted primarily from a short-lived and spatially localized region of high excitation whereas low energy protons are primarily emitted from a source of larger space-time extent, e.g. a long-lived compound nucleus.

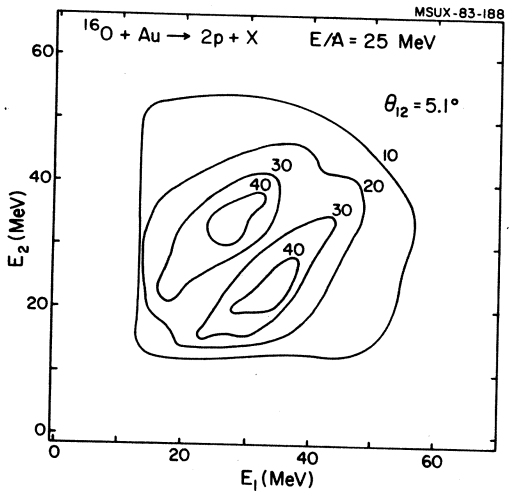

Fig.17 Contour diagram in the (E_1,E_2) plane of the proton-proton coincidence cross sections measured at an average laboratory angle of 15° for ^{16}O induced reactions on ^{197}Au at E/A=25 MeV. The coincident protons are emitted at an angular separation of θ_{12}=5.1°.

Although the observed correlations are a necessary consequence for the existence of a short lived, spatially localized region of high excitation, they cannot be considered as an unambiguous proof for the existence of a hot spot. Because of the dominance of the s-wave interaction, two-proton correlations arising from final state interactions are very similar to the ones which may result from the emission of particle unstable ^{2}He resonances[28]. Figure 17 shows a contour diagram in the (E_1,E_2) plane of the proton-proton coincidence cross sections measured[27] at an average laboratory angle of 15° for ^{16}O induced reactions on ^{197}Au at E/A=25 MeV. The qualitative features of this contour diagram illustrate in a very suggestive way that the observed correlations may also be caused by the emission of unstable ^{2}He nuclei.

The relative abundance of protons, deuterons, tritons and alpha particles can only be understood in terms of statistical calculations if the emission of ^{2}He nuclei and other particle unstable resonances from highly excited nuclear systems is included[17]. Although there are some uncertainties concerning the treatment of very broad resonances, existing statistical models[16,22] make very specific predictions about the relative abundance of bound and unbound light particles. The experimental observation of at least some of these resonances could provide a very sensitive test of the statistical treatment of noncompound light particle emission. First consistent calculations of correlations resulting from the statistical emission of nucleons, bound light nuclei, and particle unbound resonances have recently been performed for the special case of sequential particle emission from a highly excited and fully equilibrated compound nucleus[28].

For nuclear reactions involving nearly symmetric projectile target combinations, compound and noncompound light particle emission are not as clearly separated kinematically as for the case of very asymmetric target projectile combinations[10]. As a consequence, light particle spectra measured for ^{16}O induced reaction on ^{12}C and ^{27}Al are expected to contain significant contributions from the later, more equilibrated stages of the reaction[11]. In fact, the shapes of the energy spectra measured for ^{16}O induced reactions on ^{12}C at E/A=25 MeV are not inconsistent with compound nucleus emission (see also Fig. 25, below). It is, therefore, interesting to investigate whether the assumption of compound nucleus emission by itself can reproduce the proton proton correlations measured[27] for these target nuclei. The corresponding energy summed correlation functions, $1+R(\Delta p)$, are shown in Figure 18 together with calculations[28] for the idealized case of sequential particle emission, including the emission of ^{2}He, from a fully equilibrated compound nucleus. Final state interactions between particles emitted sequentially were neglected in these calculations. The agreement between theory and experiment is excellent. It should be pointed out that the correlations observed for these lighter systems are less pronounced than the correlations measured for reactions on

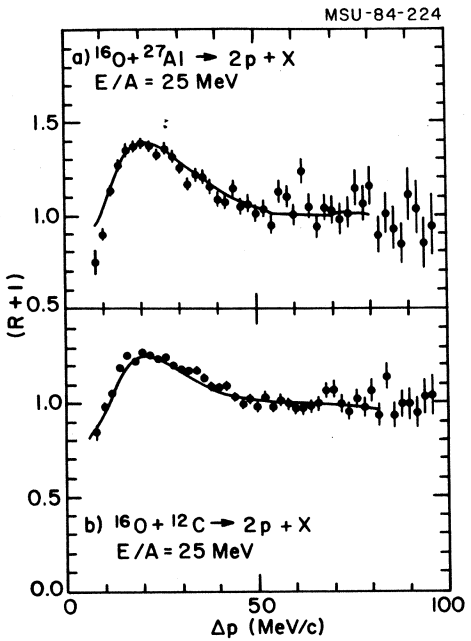

Fig.18 Two proton correlation function measured[27]) for ^{16}O induced reactions on ^{12}C and ^{27}Al at E/A=25 MeV. The curves are results of calculations[28]) for decay of the compound nucleus which include the emission and subsequent decay of ^{2}He.

^{197}Au. In terms of the final-state interaction model, this reduction of the correlations may be caused by enhanced contributions from the later, more equilibrated stages of the reaction corresponding to non-negligible source lifetimes.

For ^{16}O induced reactions on ^{197}Au, emission of ^{2}He from the compound nucleus is suppressed by the large Coulomb barrier and the lower temperature and cannot explain the measured correlations[28]). At present, we do not have a sufficiently reliable model to calculate the emission of ^{2}He prior to the attainment of full statistical equilibrium. Since the present measurements were performed at forward angles where contributions from the sequential decay of excited projectile residues are likely to be present, ^{2}He emission from excited projectile fragments cannot be excluded a priori. These contributions are difficult to assess since the excitation energies of

the primary fragments are not known. In order to eliminate contributions from the sequential decay of excited projectile residues, measurements should be performed at larger angles or, alternatively, in coincidence with fission fragments or evaporation residues.

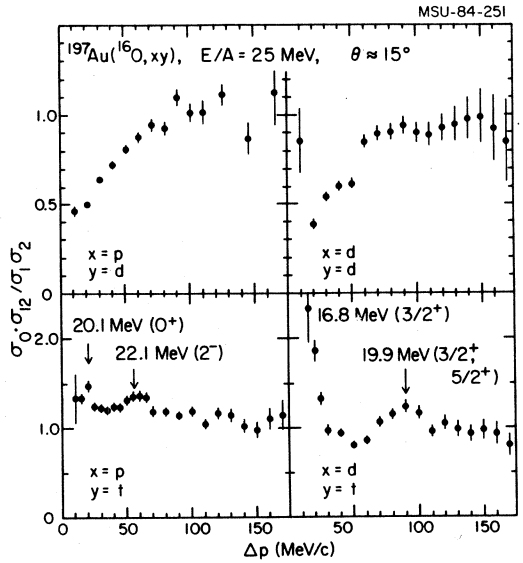

Fig.19 Light particle correlations between different hydrogen isotopes emitted at an average laboratory angle of about 15° in ^{16}O induced reactions on ^{197}Au at E/A=25 MeV. The location of some known particle unstable resonances is indicated in the figure[27]).

Light particle correlations resulting from final state interactions are expected to be most pronounced for systems with sharp resonances; they are, however, not restricted to these cases. Figure 19 shows correlations[27]) between different hydrogen isotopes emitted at an average laboratory angle of about 15° in ^{16}O induced reactions on ^{197}Au at E/A=25 MeV. For orientation, the location of some known particle unstable resonances is indicated in the figure. The strong correlations observed for deuteron-triton coincidences may be caused by either final state interactions or, alternatively, by the direct emission of highly excited ^{5}He nuclei. On the other hand, the strong suppression of the proton-deuteron and deuteron-deuteron coincidence

cross sections at small relative momenta cannot be interpreted in terms of the direct statistical emission of particle unstable resonances. Clearly, there are many open questions which will have to be addressed by future experimental and theoretical investigations. The examples given above should, however, illustrate that detailed measurements of light particle correlations at small relative momenta provide a new wealth of information about the space-time evolution of intermediate and high energy nucleus nucleus collisions. The quantitative description of light particle correlations at small angles in terms of a model which is consistent with the existing experimental information on single particle inclusive observables and which treats the emission of particle unstable resonances in addition to the uncorrelated emission of nucleons and light composite nuclei (which may or may not undergo final state interactions, depending on the space-time characteristics of the emitting source) is clearly a challenging theoretical problem for the future.

6. Azimuthal distribution of noncompound light particles

The investigation of light particle correlations at large relative momenta may provide useful information about the dynamical and geometrical aspects of the reaction. An enhanced emission of noncompound light particles in a direction perpendicular to the entrance channel scattering plane could, for example, be caused by nuclear shadowing effects[11]) or by hydrodynamic compression effects[29]) both of which should lead to the preferential emission of noncompound light particles in a plane perpendicular to the line connecting the centers of the two colliding nuclei. Only very few experiments have been performed to address these interesting questions.

First experimental evidence that nonequilibrium light particle emission in fusion-like reactions exhibits large azimuthal anisotropies was recently obtained[30]) for ^{14}N induced reactions on ^{197}Au at E/A=30 MeV. In this experiment, light particles were detected

in coincidence with fission fragments in order to (i) reduce contributions from peripheral, transfer-like reactions (for which the sequential decay of excited projectile residues might introduce trivial azimuthal asymmetries), and (ii) obtain information about the orientation of the entrance channel scattering plane (which is defined as the plane which contains the beam axis and which is perpendicular to the semiclassical angular momentum vector of relative motion between projectile and target).

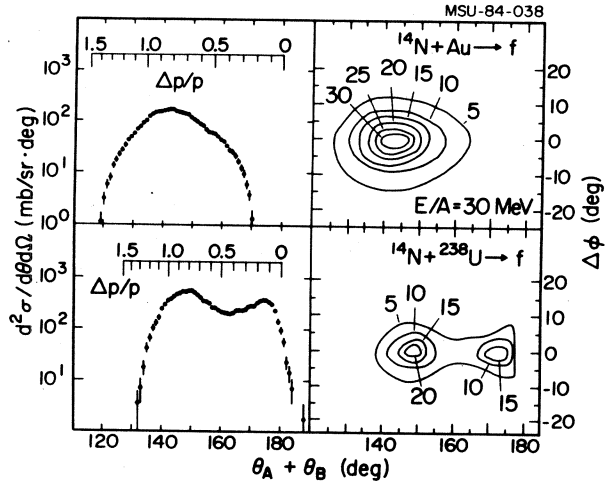

Fig.20 Comparison of folding angle distributions between coincident fission fragments measured[6],[30]) for ^{14}N induced reactions on ^{197}Au and ^{238}U at E/A=30 MeV.

For ^{14}N induced reactions on ^{197}Au, fission fragments originate primarily from fusion-like collisions for which the major part of the projectile is absorbed by the target nucleus. To illustrate this point, Figure 20 gives a comparison of the fission-fragment folding-angle distributions measured for reactions on ^{197}Au and ^{238}U. In contrast to reactions on ^{238}U, transfer-like reactions corresponding to $\theta_A+\theta_B>170°$ are strongly suppressed for reactions on ^{197}Au because of the lower fissility of the target-like residues.

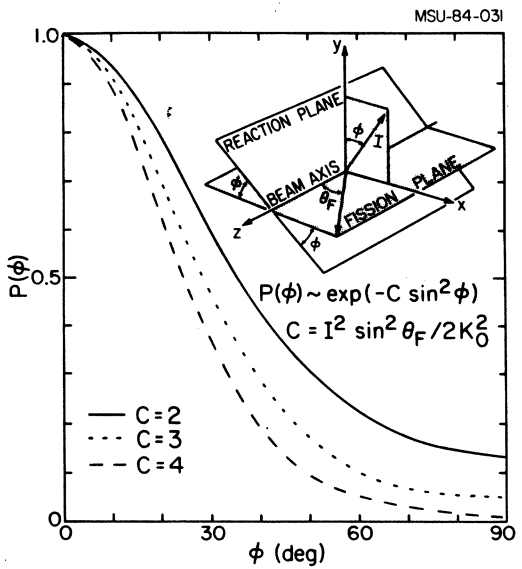

Fig. 21 Characteristic shapes of the probability distribution P(φ) for the angle φ between the fission plane and the entrance channel scattering plane.

Information about the orientation of the entrance channel scattering plane may be obtained from the fission fragments resulting from the fission decay of the heavy residual nucleus. The basic principle is illustrated in Figure 21. For simplicity, we will neglect the intrinsic spins of the projectile and target nuclei and the angular momentum of particles emitted prior to fission. In this approximation, the total angular momentum I of the fissioning nucleus is equal to the entrance channel orbital angular momentum of relative motion between projectile and target nuclei. In the absence of light particle emission, fission fragments resulting from the fission decay of the compound nucleus are emitted in a plane containing the beam axis. (Because of light particle emission, this plane is not strictly defined as is evident from the finite width of the $\Delta\phi$ distribution, see Fig. 20. Experimentally, we define the fission plane as the plane spanned by the beam axis and the velocity vector of one of the two fission fragments.) Semiclassically, the probability distribution,

$P(\phi)$, for the angle ϕ between the entrance-channel scattering plane and the fission plane may be expressed as[31]

$$P(\phi) = \text{const.}\ \exp[-C\sin^2(\phi)], \qquad (3)$$

where $C=I^2\sin^2\theta_F/2K_o^2$. Since the detailed properties of the fissioning system are not known, C cannot be specified a piori. The shapes of some reasonable distributions, corresponding to C=2,3,and 4, are shown in Fig. 2. These distributions illustrate that fission fragments are preferentially emitted in the entrance channel scattering plane.

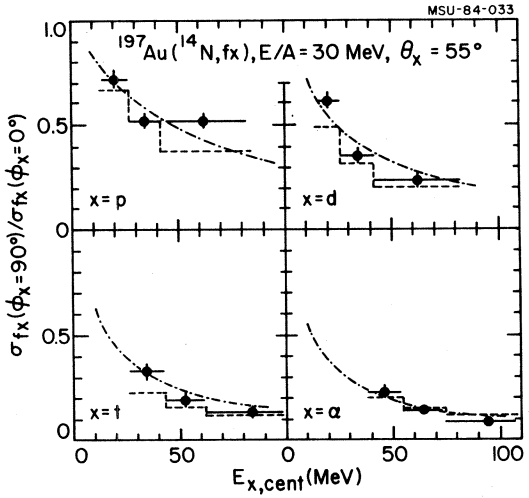

Fig.22 Ratio of out-of-plane to in-plane coincidences between fission fragments and light particles[30].

By measuring light particles in coincidence with fission fragments one may address the question whether noncompound light particles are preferentially emitted in the entrance channel scattering plane (denoted by ϕ_x=0°) or in a direction perpendicular to this plane (denoted by ϕ_x=90°). Figure 22 shows the ratios of the out-of-plane to in-plane fission-fragment light-particle coincidence cross sections. These ratios decrease significantly with increasing energy and mass of the coincident light particles indicating that noncompound

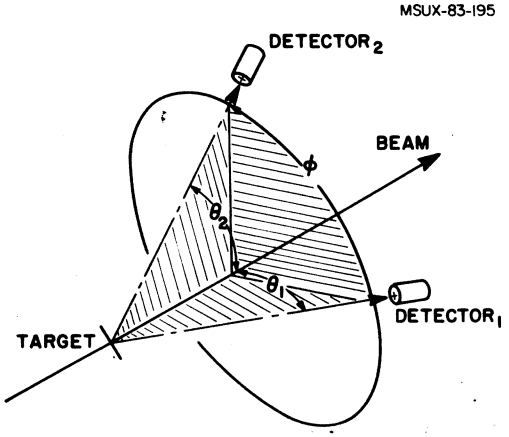

Fig. 23 Definition of angles used for the description of two-particle inclusive correlations data.

light particles are preferentially emitted in the entrance channel scattering plane. These observations differ from the qualitative expectations from nuclear shadowing[11]) or from hydrodynamic compression[29]).

An enhanced emission of nonequilibrium particles in the entrance channel scattering plane might be due to an ordered collective motion of the emitting source in this plane. For illustration, the results of two schematic calculations[30]) are shown in the figure. For the first calculation, shown by the dashed histogram, an emitting source is assumed which rotates with an angular velocity ω about an axis perpendicular to the entrance channel scattering plane while moving with a velocity v_o parallel to the beam axis. In the second calculation, shown by the dot-dashed curve, the ordered motion is assumed to be purely translational with a significant velocity component perpendicular to the beam in the entrance channel scattering plane. (For details of these calculations and the parameters used see ref. 30.) Since both of these rather simple model calculations qualitatively describe the data, it is likely that similar agreement could be obtained by other models which superimpose the random

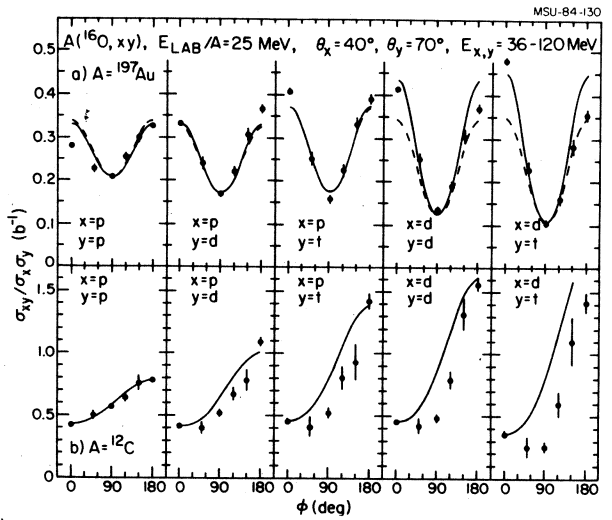

Fig.24 Azimuthal angular correlations[34]) between coincident light particles emitted at θ=40° and 70° with respect to the beam axis for ^{16}O induced reactions on ^{197}Au (a) and ^{12}C (b) at E/A=25 MeV. A low energy threshold of 36 MeV was applied. The calculations are explained in the text.

statistical motion of the participating nucleons upon a collective transverse velocity.

7. Light particle correlations at large relative momenta

Light particle correlations at large relative momenta for which final state interactions between the two detected light particles are negligible provide further information about the dynamical and geometrical aspects of the early stages of the collision process.

In order to describe the correlations between two light particles, 1 and 2, we use the angles defined in Figure 23: θ_1 and θ_2 denote the polar angles measured with respect to the beam axis and ϕ denotes the difference between the azimuthal angles of the outgoing

particle momenta.

Figure 24 shows azimuthal correlations[34]) between coincident light particles emitted to polar angles of 40° and 70° for ^{16}O induced reactions on ^{197}Au (part a) and on ^{12}C (part b). In order to reduce systematic errors, the azimuthal correlation is defined by the ratio of the coincidence cross section divided by the singles cross sections $\sigma_{xy}/\sigma_x\sigma_y$. Contributions from compound nucleus decay were reduced by applying a low energy threshold of 36 MeV in computing the cross sections. For reactions on ^{197}Au, coincident light particles are preferentially emitted in a plane which contains the beam axis. These observations are consistent with the results discussed in the previous section (see Fig. 22) where it was shown that non-compound light particles are preferentially emitted in the entrance channel scattering plane. The general trend of these azimuthal correlations can be described by assuming the superposition of a collective motion in the reaction plane on the random motion of the individual nucleons. The schematic calculations shown in Figure 24a corroborate this point. The solid curves correspond to the emission from a rotating moving source; these calculations are similar to the ones shown the dashed histogram in Figure 22. The parameterisation of purely translational motion in terms of a single sidewards deflected source results in coincidence cross sections which are left-right asymmetric. Although such a parameterisation is consistent with the data shown in Figure 22, it is not consistent with the light particle correlations shown in Figure 24a which are nearly left-right symmetric with respect to the beam axis. However, purely translational motion consistent with the measured correlations may be parameterised in terms of emission from two sources which are deflected to opposite sides of the beam axis. The results obtained with such a simple parameterisation are shown by the dashed curves in Figure 24a. (For more details of these calculations and the parameters used see ref. 34.) The overall trends of the azimuthal correlations measured for reactions on ^{197}Au is are rather well described by both parameterisations which are also in fair agreement with the singles spectra, see Figure 25. (The dashed and

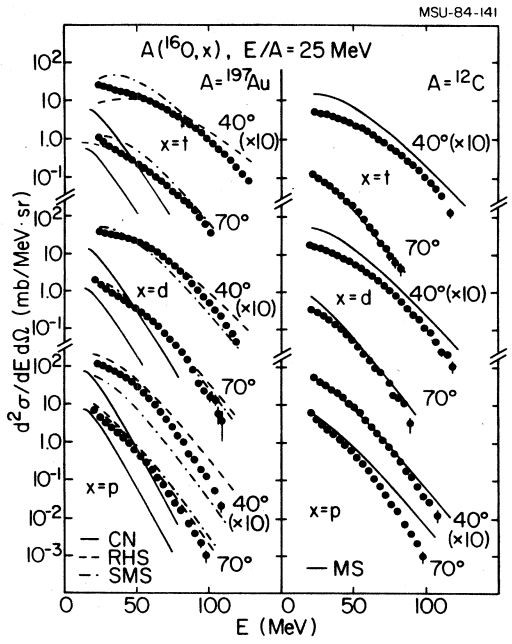

Fig.25 Inclusive light particle cross sections measured[34]) for ^{16}O induced reactions on ^{197}Au (left hand side) and ^{12}C (right hand side) at E/A=25 MeV. For reactions on ^{197}Au, estimated upper limits for contributions from compound nucleus evaporation are shown by the solid lines. The calculations are explained in the text.

dot-dashed curves in Figure 25 correspond to calculations for the rotating and the two sidewards deflected sources, respectively.) Momentum conservation and nuclear shadowing effects are expected to affect the relative magnitude of the cross sections corresponding to coincident particle emission to the same (φ=0°) and to opposite (ϕ=180°) sides of the beam axis. Since these effects are not incorporated into the two parameterisations, the relative magnitudes of these cross sections are not reproduced.

The relative success of the simple parameterisations employed in the calculations of the azimuthal light particle asymmetries may be understood in terms of the relative importance of ordered and random motion. The energy spectra of protons and composite light particles may be characterized in terms of rather similar temperature parameters, see Figure 8. Correspondingly, the "thermal" velocity

components decrease with increasing mass of the emitted particle. On the other hand, the non-random velocity components which describe the overall motion of the emitting system do not depend on the mass of the emitted particle. As a consequence, heavier particles are more sensitive to the collective motion of the emitting system since the "noise" introduced by the random velocity components is reduced.

In contrast to reactions on ^{197}Au, there is a clear enhancement for the emission of two coincident light particles to opposite sides of the beam axis for reactions induced by ^{12}C, see Figure 24b. This enhancement becomes more pronounced with increasing mass of the detected light particle. These correlations may be understood in terms of the phase space constraints imposed by momentum conservation[35]). The solid curves shown in Figure 24b illustrate the effects of momentum conservation for a source of A_s=28 nucleons and temperature T=7.1 MeV moving with the velocity of the compound nucleus, v_o=0.13c. In these calculations (and the ones shown in Figure 26 below) it is assumed that the momentum $\vec{P}_x$ of the emitted particle of mass number A_x changes the mean velocity of the second particle by $\Delta\vec{v}_o=A_x\vec{P}_x/m_x(A_s-A_x)$, i.e. the entire residual source is assumed to recoil to conserve momentum. These simple calculations reproduce the overall trend of the singles (see solid curves on the right hand side of Fig.25) and the coincidence cross sections (see solid curves in Fig.24b) rather well.

The ratios $\sigma_{xy}(\phi=180°)/\sigma_{xy}(\phi=0°)$ of the coincidence cross sections for emission to opposite sides and to the same side of the beam axis are given in Figure 26. For reactions on ^{197}Au, this ratio decreases with increasing mass of the two coincident light particles, in striking contrast to the strong increase measured for reactions on ^{12}C. The dot-dashed and dashed lines in the figure[34]) illustrate the effects due to momentum conservation assuming that momentum is conserved for subsets of A_s=28 and A_s=40,60,90, and 213 nucleons, respectively. Qualitatively, these observations might be explained in terms of the competing effects caused by shadowing and momentum conservation. If particle emission prior to the attainment of full statistical equilibrium of the composite system originates from a

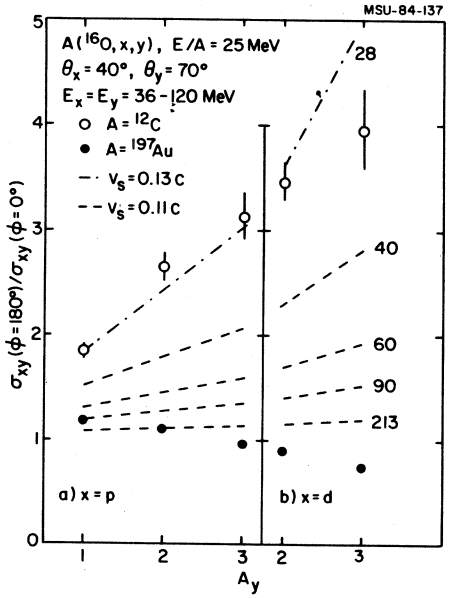

Fig.26 Ratio of cross sections corresponding to emission of coincident light particles to opposite sides and to the same side with respect to the beam axis for ^{16}O induced reactions on ^{12}C (open points) and ^{197}Au (full points) at E/A=25 MeV. The dashed and dot-dashed curves illustrate the effects of momentum conservation for systems with finite numbers of nucleons[34]).

localized region of high excitation, absorption or rescattering by the adjacent spectator nuclear matter will enhance emission to the same side of the beam axis. Momentum conservation, on the other hand, will favor emission to opposite sides of the beam axis. Whether coincident light particles are preferentially emitted to the same or to opposite sides of the beam axis will depend on the relative magnitude of these effects. Absorptive effects are expected to be more pronounced for the emission of composite light particles than for the emission of nucleons. This is in qualitative agreement with the trends measured for reactions on ^{197}Au where it is observed that coincident protons have a slight preference to emerge at opposite sides of the beam axis, whereas coincident composite light particles have a slight preference to emerge at the same side of the beam axis.

8. Conclusion

Intermediate and high energy nucleus nucleus collisions are characterized by particle emission prior to the attainment of full statistical equilibrium of the composite nuclear system. Many single particle observables may be rather well described in terms of statistical approaches which are based on the assumption that only subsets of nucleons participate in the early stages of the interaction for which the kinetic energy per participating nucleon is high. Important questions concern the spatial localization of excitation energy and the possible attainment of local statistical equilibrium. Detailed investigations of light particle correlations at small relative momenta may provide useful information about the space-time evolution of the reaction. First results from two-proton correlation measurements are consistent with the emission of energetic light particles from a localized region of high excitation. However, alternative interpretations cannot be ruled out and should be investigated. Ultimately, light particle correlations at small relative momenta may provide severe constraints for models which are capable of treating the emission of nucleons, bound light particles and particle unstable resonances as well as final state interactions among the emitted particles.

Light particle correlations at large relative momenta may provide additional information about the geometrical and dynamical aspects of the reaction. Because of the importance of phase space constraints imposed by conservation laws on small subsets of nucleons, the description of two-particle observables will require theories which take these conservation laws into account. There is a clear need for a more fundamental treatment of intermediate energy nucleus nucleus collisions in terms of theories which incorporate the effects of the mean nuclear field (which cannot be expected to be negligible at intermediate energies) as well as the effects of individual nucleon nucleon collisions (for which the appropriate treatment of Fermi motion and Pauli blocking presents a nontrivial problem).

In this talk I have focussed the discussion on a kinematical region where simple processes such as direct transfer-like reactions followed by the sequential decay of excited projectile residues or direct knockout reactions are expected to be less important and where statistical concepts might be applicable. Whether these more violent collisions may eventually be used to study the properties of highly excited nuclear matter is still an open question. It should, however, be clear that inferences about the properties of nuclear matter can only be made if the dynamical and statistical processes which determine collisions of finite nuclei are understood in detail.

Acknowledgements

It is a pleasure to acknowledge the invaluable contributions of C.B. Chitwood, D.J. Fields, W.G. Lynch, and M.B. Tsang. This material is based upon work supported, in part, by the National Science Foundation under Grant No. PHY-83-12245.

References

1) M.W. Curtin, H. Toki, and D.K. Scott, Phys. Lett. 123B (1983) 289

2) H. Morgenstern, W. Bohne, K. Grabisch, D.G. Kovar, and H. Lehr, Phys. Lett. 113B (1982) 463

3) H. Morgenstern, W. Bohne, W. Galster, K. Grabisch, and A. Kyanowski, Phys. Rev. Lett. 52 (1984) 1104

4) T. Sikkeland, E.L. Haines, and V.E. Viola, Jr., Phys. Rev. 125 (1962) 1350

5) V.E. Viola, Jr., B.B. Back, K.L. Wolf, T.C. Awes, C.K. Gelbke, and H. Breuer, Rev. C26 (1982) 178

6) M.B. Tsang, D.R. Klesch, C.B. Chitwood, D.J. Fields, C.K. Gelbke, W.G. Lynch, H. Utsunomiya, K. Kwiatkowksi, V.E. Viola, Jr., and M. Fatyga, Phys. Lett. 134B (1984) 169

7) B.B. Back, K.L. Wolf, A.C. Mignerey, C.K. Gelbke, T.C. Awes, H. Breuer, V.E. Viola, Jr., and P. Dyer, Phys. C22 (1980) 1927

8) J. Kasagi, S. Saini, T.C. Awes, A. Galonsky, C.K. Gelbke, G. Poggi, D.K. Scott, K.L. Wolf, and R. Legrain, Phys. Lett. 104B (1981) 434

9) T.C. Awes, G. Poggi, C.K. Gelbke, B.B. Back, B.G. Glagola, H. Breuer, and V.E. Viola, Jr., Phys. Rev. C24 (1981) 89

10) T.C. Awes, S. Saini, G. Poggi, C.K. Gelbke, D. Cha, R. Legain, and G.D. Westfall, Phys. Rev. C25 (1982) 2361

11) W.A. Friedman, Phys. Rev. C29 (1984) 139

12) T. Udagawa and T. Tamura, Phys. Rev. Lett. 45 (1980) 1311

13) T. Udagawa, D. Price, and T. Tamura, Phys. Lett. 116B (1982) 311

14) G.D. Westfall, B.V. Jacak, N. Anantaraman, M.W. Curtin, G.M. Crawley, C.K. Gelbke, B. Hasselquist, W.G. Lynch, D.K. Scott, M.B. Tsang, M.J. Murphy, T.J.M. Symons, R. Legrain, and T.J. Majors, Phys. Lett. 116B (1982) 118

15) J. Gosset, H.H. Gutbrod, W.G. Meyer, A.M. Poskanzer, A. Sandoval, R. Stock, and G.D. Westfall, Phys. Rev. C16 (1977) 629

16) J. Gosset, J.I. Kapusta, and G.D. Westfall, Phys. Rev. C18 (1978) 844

17) C.K. Gelbke, Nucl. Phys. A400 (1983) 473c

18) J. Aichelin and G. Bertsch, Phys. Lett. 138B (1984) 350

19) J. Aichelin, Phys. Rev. Lett. 52 (1984) 2340

20) R. Shyam and J. Knoll, GSI preprint, 1984, to be published

21) D.H.E. Gross, L. Satpathy, M. Ta-chung, and M. Satpathy, Z. Phys. A309 (1982) 41

22) W. Friedman and W.G. Lynch, Phys. Rev. C28 (1983) 16, 950

23) C.B. Chitwood, D.J. Fields, C.K. Gelbke, W.G. Lynch, A.D. Panagiotou, M.B. Tsang, H. Utsunomiya, and W.A. Friedman, Phys. Lett. 131B (1983) 289

24) D.J. Fields, W.G. Lynch, C.B. Chitwood, C.K. Gelbke, M.B. Tsang, H. Utsunomiya, and J. Aichelin, to be published

25) G.I. Kopylov, Phys. Lett. 50B (1974) 472

26) S.E. Koonin, Phys. Lett. 70B (1977) 43

27) W.G. Lynch, C.B. Chitwood, M.B. Tsang, D.J. Fields, D.R. Klesch, C.K. Gelbke, G.R. Young, T.C. Awes, R.L. Ferguson, F.E. Obenshain, F. Plasil, R.L. Robinson, and A.D. Panagiotou, Phys. Rev. Lett. 51 (1983) 1850, and to be published

28) M.A. Bernstein, W.A. Friedman, and W.G. Lynch, Phys. Rev. C29 (1984) 132, and private communication

29) M.I. Sobel, P.J. Siemens, J.P. Bondorf, and H.A. Bethe, Nucl. Phys. A251 (1975) 502

30) M.B. Tsang, C.B. Chitwood, D.J. Fields, C.K. Gelbke, D.R. Klesch, W.G. Lynch, K. Kwiatkowski, and V.E. Viola, Jr., Phys. Rev. Lett. 52 (1984) 1967

31) L.C. Vaz and J.M. Alexander, Phys. Rep. 97 (1983) 1

32) T. Ericson and V. Strutinski, Nucl. Phys. 8 (1958) 284

33) I. Halpern, unpublished

34) M.B. Tsang, W.G. Lynch, C.B. Chitwood, D.J. Fields, D.R. Klesch, C.K. Gelbke, G.R. Young, T.C. Awes, R.L. Ferguson, F.E. Obenshain, F. Plasil, and R.L. Robinson, to be published

35) W.G. Lynch, L.W. Richardson, M.B. Tsang, R.E. Ellis, C.K. Gelbke, and R.E. Warner, Phys. Lett. 108B (1982) 274